RSC Advances

PAPER

View Article Online
View Journal | View Issue

Cite this: *RSC Adv.*, 2020, **10**, 5894

Synthesis, characterization and antifungal activities of eco-friendly palladium nanoparticles†

Francis J. Osonga,‡[a] Sanjay Kalra,[a] Roland M. Miller,[a] Daniel Isika[b] and Omowunmi A. Sadik *[b]

Palladium is a versatile catalyst, but the synthesis of palladium nanoparticles (PdNPs) is usually attained at a high temperature in the range of 160 °C to 200 °C using toxic reducing agents such as sodium borohydride. We report the synthesis of PdNPs using a low-cost and environmentally-friendly route at ambient temperatures. Quercetin diphosphate (QDP), a naturally-derived flavonoid, was employed as a reducing, capping, and stabilizing agent. The effect of temperature was optimized to produce perfectly spherical PdNP nanoparticles with sizes ranging from 0.1 to 0.3 microns in diameter. At relatively higher concentration of QDP, significantly smaller particles were produced with a size distribution of 1–7 nm. Perfectly spherical PdNP nanoparticles are a rare occurrence, especially under ambient room temperature conditions with fast reaction time. The formation of the nanoparticles was confirmed using UV-vis, TEM, EDS, and XRD. HRTEM demonstrated the lattice structure of the PdNPs. The synthesized PdNPs were also tested for their antifungal properties against *Colletotrichum gloeosporioides* and *Fusarium oxysporum*. Results showed that the size of the PdNPs played a critical role in their antifungal activity. However, for *F. oxysporum*, other factors beyond size could affect the antifungal activity including fine-scale, nutrient composition, and target organisms.

Received 25th September 2019
Accepted 23rd January 2020

DOI: 10.1039/c9ra07800b

rsc.li/rsc-advances

1 Introduction

Palladium nanoparticles, with their seemingly endless potentials as electrocatalysts, often experience a common occurrence of poisoning. During the initial synthesis of palladium nanoparticles (PdNPs), reducing, stabilizing, and capping agents are used to stimulate and control growth, however these reagents are often harmful organic solvents, surfactants, and toxic chemicals.[1–5] The use of these reagents, while effective at morphology control and synthesis, promote catalyst poisoning. Greener synthesis of PdNPs could provide a viable approach to combat catalyst poisoning and degradation.

Palladium has a configuration of $4d^{10}5s^{0}$. The unique empty 5s shell allows the element to be less dense and have the lowest melting point out of all of the platinum group metals. When excited, it's surface plasmon resonance (SPR) has proved useful in sensing, chemical optical transducers, and plasmonic waveguiding.[6,7] PdNPs are a versatile catalyst. Its high surface-to-volume ratio is excellent for homogenous and heterogeneous catalysis, low selective oxidation of alkanes, hydrogenation of alkynes to alkenes without further reduction into alkanes, catalysis of carbon–fluorine (C–F) bonds, and last but not least, Suzuki coupling reactions and its many variations.[4–8]

The synthesis of PdNPs is performed in one of two environments, free and confined space settings. The free space synthesis is achieved using methods such as sonochemistry, electrochemistry, wet chemistry, biological molecules, and reactive micelles.[9,10] The confined space methods include dendrimer synthesis, mesoporous materials, and reverse micelle synthesis. Essentially, nanoparticles are formed *via* the reduction of the corresponding metal salt ($PdCl_2$ in the case of PdNPs) encapsulated within a specific stabilizer. At the early stage of nucleation, the metal ion is reduced to a zero-valent metallic state, while metal atoms collide with ambient atoms to create clusters and provide seeds for the subsequent growth of particles.[11,12] Due to the difficult stabilization of noble metal nanoparticles, palladium is stabilized by thiols, phosphines, phenanthroline, and chiral diphosphite. Protective groups, agents with electrostatic and steric effects based on different stabilization modes, are widely used to control nanoparticle size.[20] Although chemical synthesis of PdNPs is widely accepted and used, there are several problems associated with the endeavor. The overall process is expensive, sensitive to air or moisture ligands, uses toxic organic solvents, has unacceptably

[a]*Department of Chemistry, Center for Research in Advanced Sensing Technologies & Environmental Sustainability (CREATES), State University of New York at Binghamton, P. O. Box 6000 Binghamton, NY, 13902, USA*

[b]*Department of Chemistry and Environmental Science, New Jersey Institute of Technology, University Heights, Newark, NJ, 07102, USA. E-mail: sadik@njit.edu*

† Electronic supplementary information (ESI) available. See DOI: 10.1039/c9ra07800b

‡ Present address: Ralph E. Martin Department of Chemical Engineering, University of Arkansas, 3202 Bell Engineering Center, Fayetteville, Arkansas 72701, USA.

low yields, low catalytic efficiencies, a high leaching of metal species, long reaction times, short storage life, and a lack of size control on the particles. The recovery and reusability of catalysts is a very important factor when dealing with noble metals in C–C coupling reactions such as Suzuki–Miyaura cross-coupling reactions; chemically synthesized PdNPs have shown to be unrecyclable and often unrecoverable, making them very expensive to use as reagents & catalysts regularly.[9–11]

In comparison to synthetic chemical approaches of producing PdNPs, greener synthesized particles do not require high temperatures, toxic organic solvents, and long synthesis times. These particles have also been reported to remain stable for three times as long as non-green methods. Synthesis of PdNPs using *H. rhamnoides* has resulted in particles that remain stable over a month after synthesis with no change or degradation in morphology.[12–15] Naturally-occurring phenols in flavonoids are believed to donate electrons to the metal-ion complex and act as the true reducing agents for this process.[13–17] It has been reported that pi-electrons of the carbonyl group (C=O) from the C ring in flavonoids can transfer electrons to the free 5s orbital of the metal ion and convert the species into a free metal. We have previously explored the use of water-soluble quercetin pentaphosphate (QPP), a naturally-occurring derivatized flavonoid in the immobilization of lead[18] by creating a metal complex and rendering lead less available in the environment. QPP is non-toxic, and complexes with metals under ordinary surrounding conditions and has been used effectively in the synthesis of silver and gold nanoparticles.[19,20] Organic solvents used as capping and reducing agents can be avoided by using QPP as a substitute, a molecule that has surpassed the efficiency and quality of products produced by organic solvents.

The antimicrobial properties of PdNPs are rarely studied. However, there are a few studies that have been conducted on PdNPs for their antimicrobial capabilities.[21–24] Tahir *et al.* demonstrated the use of biosynthesized PdNPs as antibacterial compounds against *Pseudomonas aeruginosa*.[21] Smaller and spherical nanoparticles were observed to have more antibacterial effects compared to larger and irregular shaped nanoparticles.[21] At 10^{-9} M concentration, Pd has also been reported to exhibit toxicity against Gram-positive bacteria such as *Staphylococci*, while at concentrations above 10^{-9} M, it exhibits toxicity towards Gram-negative bacteria.[23]

Two fungi, *Aspergillus flavus* and *Candida albicans* have previously been tested against PdNPs as well.[22] PdNPs synthesized from *Terminalia bellirica* have also been tested for their antifungal properties against *Aspergillus niger*.[24] The zone of inhibition for the PdNPs was 16 mm which was greater than the chloramphenicol (14 mm).[24] In our study, we looked at two pathogenic fungi that have global impacts, *Colletotrichum gloeosporioides*, and *Fusarium oxysporum*. In a 2012 survey of molecular plant pathologists, *Fusarium oxysporum* and *Colletotrichum* spp. were rated in the 'Top 10' of most important plant pathogens.[25] These pathogens have been implicated as the causative agents in anthracnose disease commonly reported in tubers, and other diseases of the sweet yam population that is the staple crop in Jamaica. The sweet yam production was decreased by about 70% in the last decades due to these diseases. Finding a solution to this problem would help numerous farmers and Jamaica as a whole.

We report for the first time; the synthesis of PdNPs using water-soluble phosphorylated quercetin known as quercetin diphosphate (QDP). QDP was used as a reducing and capping agent in the synthesis of PdNPs. Furthermore, the present study investigates the antifungal potential of the QDP derived PdNPs against *F. oxysporum* and *C. gloeosporioides*.

2 Materials and methods

2.1 Materials

All reagents purchased were of analytical or reagent grade purity and were used as purchased. Anhydrous *N*,*N*-dimethylformamide (DMF, 99.8%) was obtained from Acros Organics, a division of Thermo Fischer Scientific. Quercetin was purchased from Indofine Chemicals Inc. (Hillsborough, NJ). Palladium(II) chloride ($PdCl_2$), 4-dimethyl aminopyridine (DMAP), TMS-bromide were purchased from Sigma-Aldrich, Milwaukee, WI. *N*,*N*-Diisopropylethylamine (DIPEA), acetonitrile, dichloromethane, dibenzyl phosphite, carbon tetrachloride (CCl_4), were purchased from Sigma (St. Louis, MO). Dimethyl sulfoxide-D6 was from Cambridge Isotope Laboratories, Inc. MA. Potassium dihydrogen phosphate (KH_2PO_4), anhydrous sodium sulfate (Na_2SO_4), sodium chloride (NaCl), ethyl acetate, hexane and methanol were purchased from Fisher Scientific, Pittsburg, PA. Nano pure water with a specific resistivity of 18 MΩ cm was used in the preparation of reagents. All the reactions involving moisture or air-sensitive reagents were carried out under Ar or N_2 atmosphere.

2.2 Instrumentation

Transmission electron microscopy (TEM) measurements were carried out on a JEOL TEM 2100F. The TEM analysis of PdNP was achieved by adding a drop of the samples to the carbon-coated copper grid and then dried. UV/vis absorption spectra were conducted using HP 8453 UV-visible diode array spectrophotometer. XRD study was carried out using D8 Advance 800234-X-ray (9729) Bruker at 40 kV and 40 mA.

2.3 Synthesis of quercetin 5,4′-diphosphate (QDP)

Selective phosphorylation of quercetin ($C_{15}H_{10}O_7$), a plant polyphenol from the flavonoid group, found in many fruits, vegetables, leaves, and grains was performed through the installation of phosphate groups on selected hydroxyl group. In this work, the design and synthetic strategies for the sequential protection of the –OH groups were adopted to produce quercetin diphosphate. The sequential synthesis was undertaken to develop modified hydroxyl groups, which produced modified flavonoids derivatives, quercetin diphosphate (5,4′-QDP) which was synthesized and characterized as reported in our previous work.[26]

2.4 Synthesis of PdNPs

In this work, a one-pot technique was used for the duration of nanoparticle synthesis experiments. 5 mM of quercetin diphosphate (QDP) and the palladium metal precursor, 1 mM $PdCl_2$, in water were the only two reagents combined within a 20 mL glass vial. In a typical synthesis reaction, ratios were varied for 1 mM $PdCl_2$ and were reacted with constant 5 mM QDP for 5 hours at room temperature to form palladium nanoparticles. On the other hand, ratios were varied for 5 mM QDP was reacted with constant 1 mM $PdCl_2$ for 5 hours at room temperature to form palladium nanoparticles. The effect of temperature was investigated for a reaction of QDP : $PdCl_2$ at a reaction of 1 : 1 at temperatures ranging from 25–100 °C. Several trials were conducted with two experiments in mind, one to vary only the concentration under ambient room temperatures and the other to vary temperatures while keeping the concentrations constant (Tables 1 and 2). These two phases were then sampled using UV-visible spectroscopy to analyze concentrations of the resulting synthesized PdNPs. Previous literature has shown PdNPs to be apparent under UV-vis at ~430 nm wavelength.[10]

2.5 Antifungal activity of PdNPs

The well diffusion method was used in this study to investigate the antifungal activity of QDP derived PdNPs. The fungal strains, *F. oxysporum* (isolated from sweet yams and genetically identified using the internal transcribed spacer (ITS) region with 100% conformity to NCBI database algorithm) and *C. gloeosporioides* (purchased from the ATCC (MY-58221)) were used as test organisms. Fresh Potato Dextrose Agar (PDA) plates were spread plated with *C. gloeosporioides* (10^5 spores) or *F. oxysporum* (10^5 spores) under sterile conditions. Three 6 mm wells were punched in the agar of each plate and filled with 50 μL of the nanoparticle solution, aseptically.[21,27] The plates were incubated at 25 °C in the dark and observed after 1, 2, 4, and 7 days. The inhibition of fungal growth around each well was measured in 3 places and the average was calculated.

3 Results and discussion

3.1 Effect of concentration of QDP on the formation of PdNPs

PdNPs synthesis was identified and characterized with respect to constant temperatures and varying reagent concentrations, in this phase of the study. After completing several trials with a variety of concentrations (Table 1), UV-visible spectroscopy was used to monitor the synthetic process as well as identify the relative concentrations of the synthesized PdNPs between each vial. The surface plasmon resonance (SPR) peak for PdNPs was observed at 430 nm. Fig. 2 shows that a clear and distinct trend was present, as $PdCl_2$ concentrations increased while maintaining constant QDP concentrations.

Table 1 Typical experimental set-up for PdNP synthesis using varying QDP (right) and metal precursor (left)

Sample	QDP (μL)	$PdCl_2$ (μL)	Sample	QDP (μL)	$PdCl_2$ (μL)
1	400	200	1	200	400
2	400	400	2	400	400
3	400	600	3	600	400
4	400	800	4	800	400
5	400	1000	5	1000	400

Table 2 Temperature-dependent study on constant concentrations of QDP and $PdCl_2$ with six trials

Sample	Temperature (°C)	QDP (μL)	$PdCl_2$ (μL)
1	25	300	300
2	40	300	300
3	60	300	300
4	80	300	300
5	90	300	300
6	100	300	300

This implies that since there are a higher number of $PdCl_2$ molecules present (when using a higher concentration), there is a higher likelihood of QDP interactions with the available palladium ions (Fig. 1). Fig. 1 also shows a qualitative color change (right), R_0–R_5 vials represent increasing heat exposure vials with constant reagent concentrations. A clear color change occurred from pale yellow to dark brown this signaling the formation of PdNPs. The formation of nanoparticle was seen as small clusters of black particulate in each vial solution; however, R_5 had the highest colorimetric change and thus implies the highest nanoparticle production. When comparing increasing palladium precursor levels to increasing QDP levels, one can observe the same relationship. As QDP levels rose with respect to constant $PdCl_2$ molecules, the overall PdNPs production increased dramatically. In similar logic, an increase in QDP molecules ensured that more $PdCl_2$ molecules interacted, thus ensuring a more efficient PdNPs production (Fig. 2).

3.2 Effect of temperature on the formation of PdNPs

As a primary factor of reaction kinetics, temperature was tested as a variable for several one-pot method trials of QDP and $PdCl_2$. Utilizing pre-existing mechanics of heat and reaction efficiencies, the production of PdNPs was directly linked to an increase in temperature. As temperature increased from ambient 25 °C to 100 °C, vibratory characteristics of all molecules increased as well, creating an increased probability of molecular collision with overall success of product formation (Fig. 3). Observed at 430 nm, PdNPs were found in significantly higher concentrations with each successive vial as temperature increased. The maximum efficiency of nanoparticle synthesis was observed at 100 °C. This temperature study further underscores the significance of preparing efficient PdNPs under ambient conditions using QDP.

3.3 TEM characterization

Transmission electron microscopes were used during the characterization of the synthesized PdNPs from QDP. To

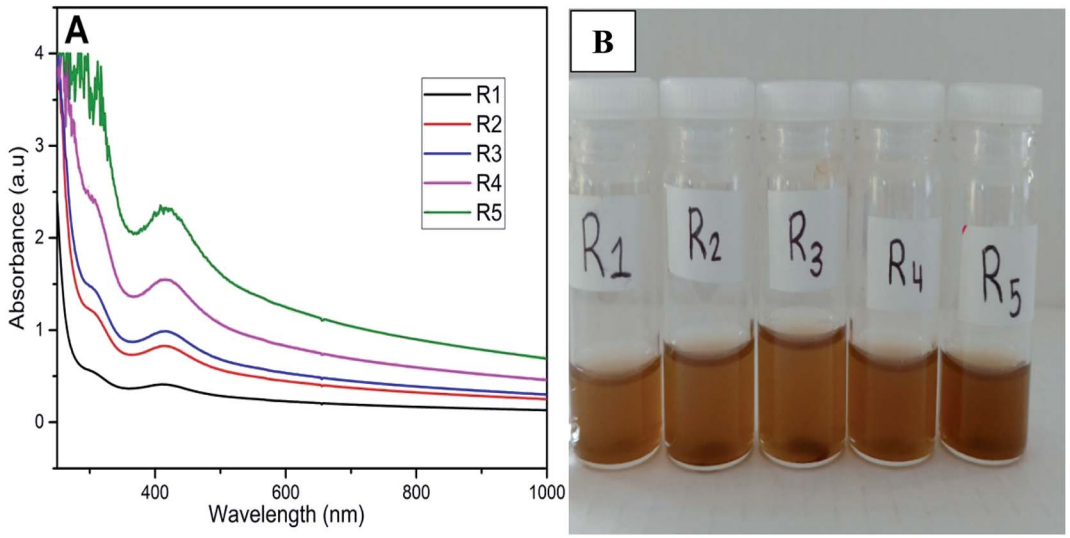

Fig. 1 (A) UV-vis spectra for the formation on PdNPs at room temperature after 8 h (right). (B) Image on the left shows the color change from clear to dark brown indicating PdNPs formation.

identify the morphology and size of each nanoparticle, TEM images were taken directly after the synthesis. An advantage of the green synthesis of PdNPs is that the reactions result in a wide array of nanoparticle sizes, however, spherical nanoparticles were the main morphology found (Fig. 4). Clearly shown in Fig. 4, PdNPs synthesized from QDP produced sizes within 0.1 to 0.8 μm in diameter (Fig. 4).

Fig. 5 represents another set of TEM data depicting the formation of spherical PdNPs within a size distribution range of 0.1 to 0.3 μm in diameter. This consistent NPS production shows that the green synthesis of palladium using QDP yields spherical particles with a narrow size range. Also, the use of QDP provides a green synthesis of palladium under room temperatures at fast reaction time. Fig. 5 depicts the PdNPs reaction using QDP under relatively low concentrations of QDP (under 600 μL). The size distribution here represents the presence of large PdNPs with perfectly spherical morphology. The perfectly spherical nanoparticles are a rare occurrence, especially under ambient room conditions and under an immediate reaction time.

When comparing QDP concentrations in this study, both relatively high (>600 μL), and relatively low (<600 μL) reagent concentrations were tested for the physical morphology of the PdNPs produced. A key idea supported by this data is that as relatively high QDP concentrations were used, significantly smaller particles were produced (Fig. S1†), the size distribution of 1–7 nm was identified. The TEM images show that the perfectly spherical morphology was still intact, yet there was some particle agglomeration due to the small size of each nanoparticle.

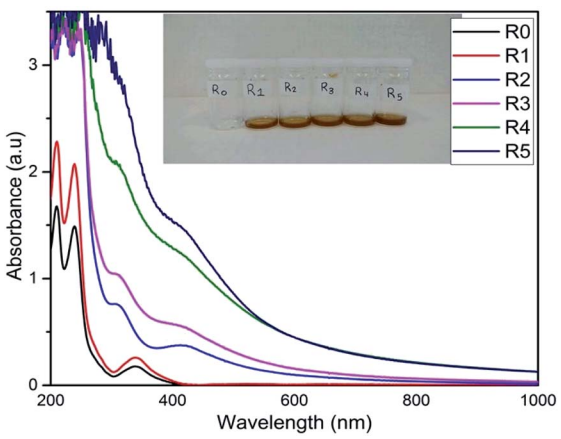

Fig. 2 Concentration dependent studies with increasing QDP concentrations R_0–R_5 (R_0 was the control, QDP). Plot shows PdNPs production at SPR peak 430 nm.

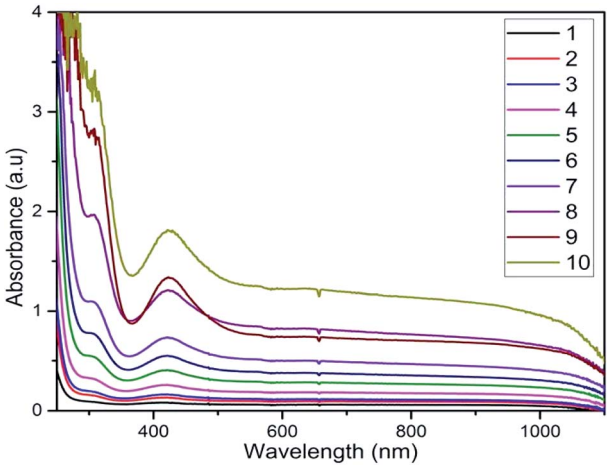

Fig. 3 Temperature dependent studies with constant concentrations and increasing temperatures as vial numbers 1 to 10. Starting at room temperature (1) to 100 °C (10).

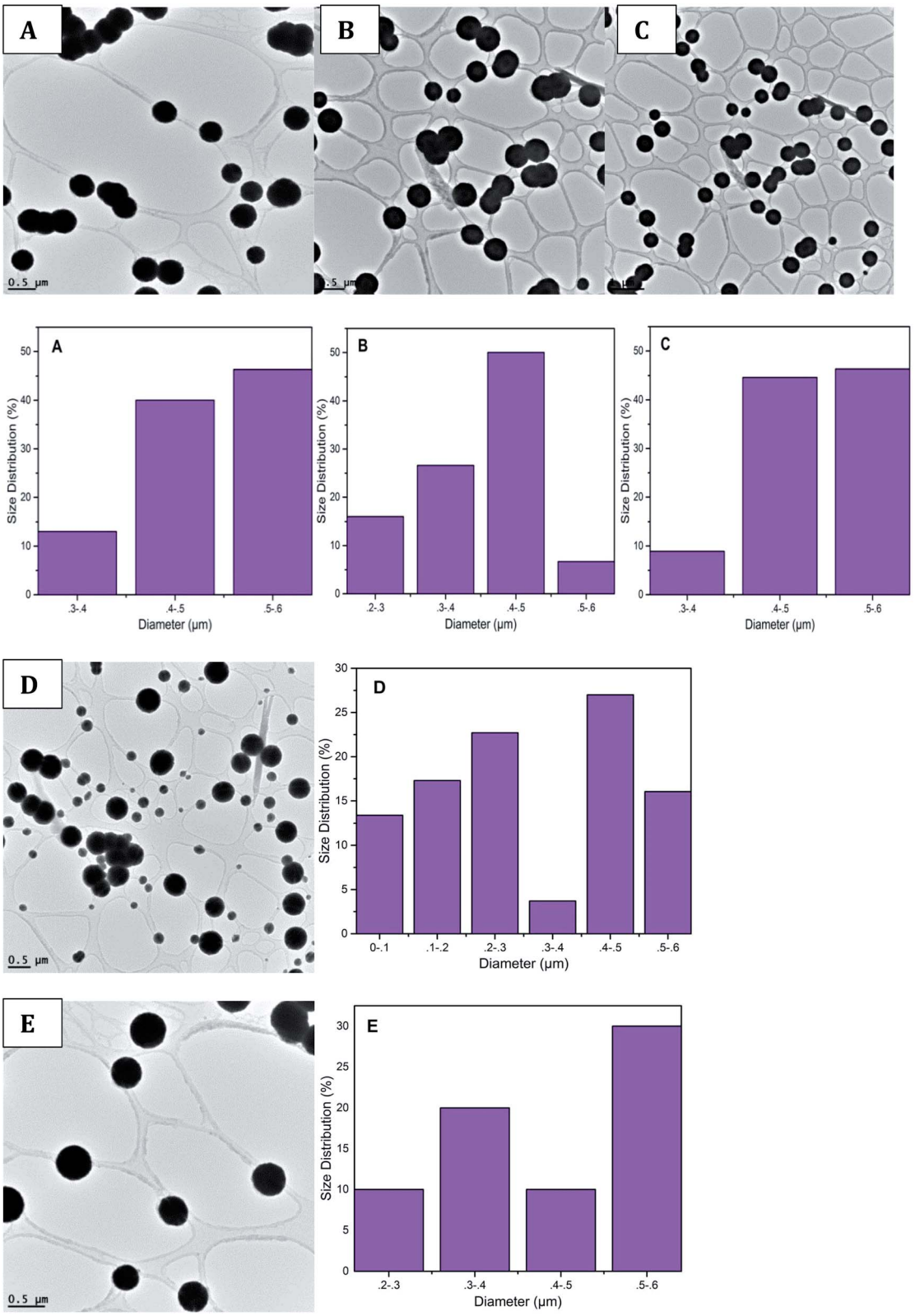

Fig. 4 TEM images, along with corresponding size distributions are shown. (A)–(E) show a size distribution of 0.3–0.8 μm in diameter.

The ability to control the size of nanoparticles using various concentrations of QDP is a novel approach to nanoparticle synthesis. Using no temperature catalyst, and under immediate reaction times, nanoparticles of perfect spherical morphology and size distributions of 0.1–0.3 μm and 1–8 nm in diameter were identified with this green synthesis.

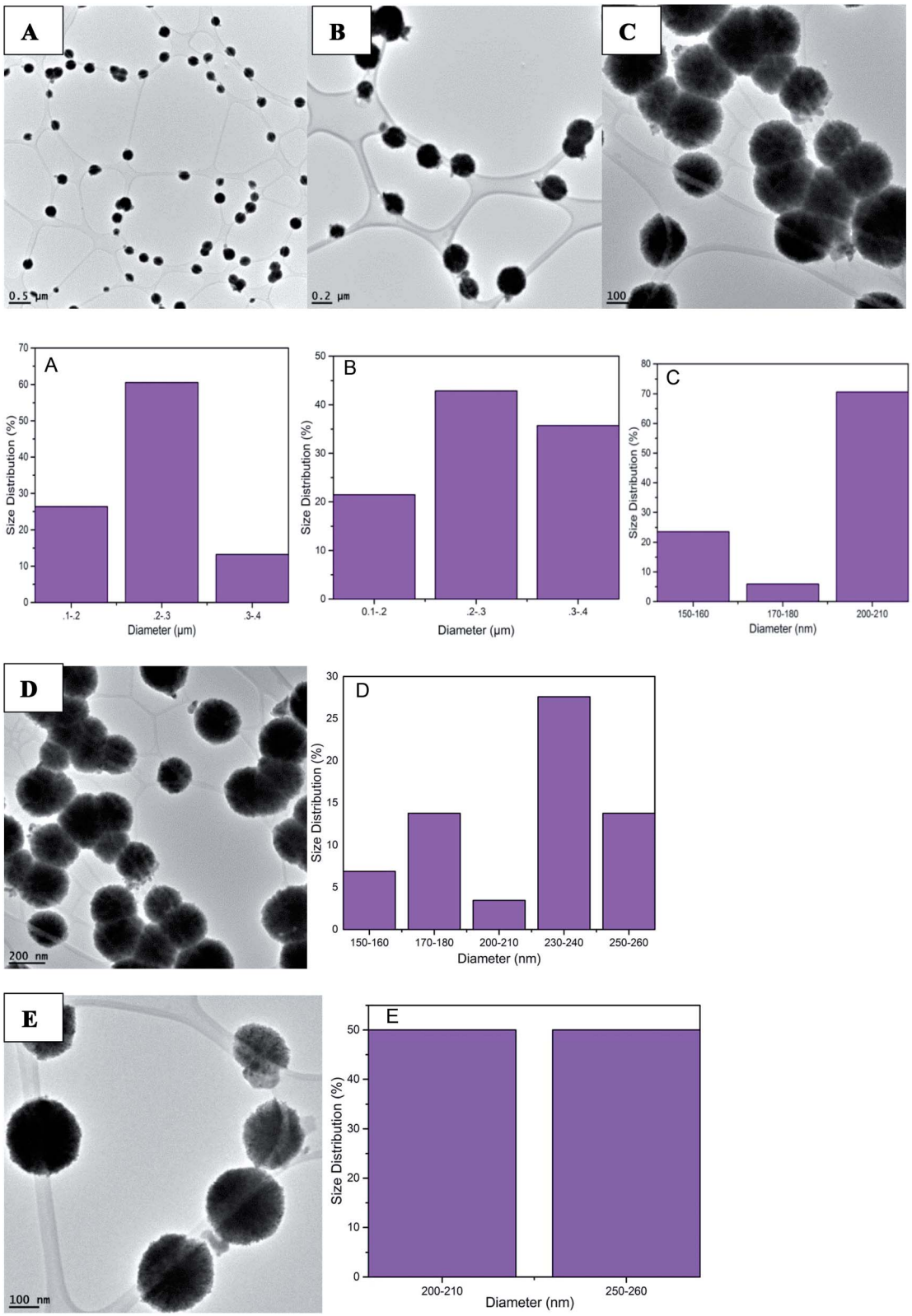

Fig. 5 TEM images of PdNPs synthesized from QDP green synthesis. Spherical NPs were found as well as the size distribution of 0.1 to 0.3 micrometers.

3.4 EDS and XRD characterization

The EDS elemental analysis was carried by scanning on a single particle and the observed characteristic peak assigned to palladium, as shown in Fig. 6(B), thus confirming the formation of elemental palladium. The HRTEM Fig. 6(A) clearly demonstrated the lattice structure of the PdNPs.

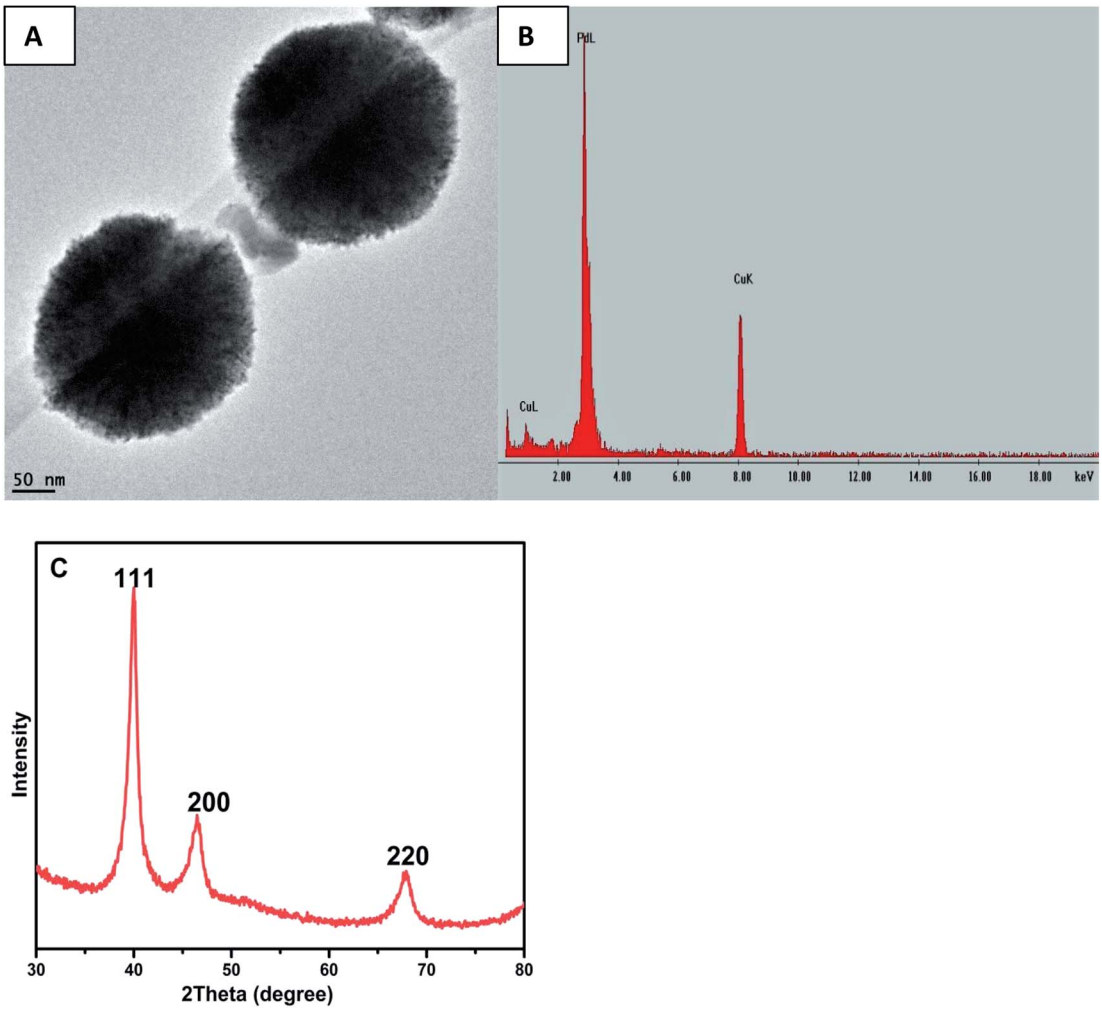

Fig. 6 HRTEM (A), EDS (B), and XRD (C) of PdNPs.

The crystalline nature of PdNPs was determined by conducting powder XRD experiments and the corresponding XRD pattern, as depicted in Fig. 6(C). The peaks $2\theta = 40.10°$, 46.25° and 67.60° are assigned to (111), (200) and (220) respectively which was comparable to JCPDS standard number 05-0681 for PdNPs and in agreement with literature values[12,16,28] thus confirming the formation of PdNPs with face-centered cubic (fcc) crystal structure. (111) Facets primarily dominated the PdNPs, and hence, the (111) planes are, therefore, the preferentially oriented growth direction.

3.5 Proposed mechanism of interaction between QDP and palladium

The synthesized quercetin derivative, QDP,[26] served multiple purposes in the synthesis of the palladium nanoparticles from palladium(II) ions. This molecule has favorable properties that facilitate its use as a reducing, capping, and stabilizing agent in the nanoparticle synthesis. For example, QDP has both C- and P-bound hydroxyl groups. These groups can freely chelate with the palladium(II) ions.[29] The nanoparticle synthesis proceeds through a couple of intermediate steps;[30] the possible final step can be represented as a redox reaction, as shown in Scheme 1. The rate and viability of the chelation of the metal ion by the hydroxyl groups is a factor of both the acidity and the steric effects of the QDP molecule.[31] Steric hindrance reduces the viability of the metal chelation process while low acidity will result in a reduced rate of hydroxyl group deprotonation, which is a key step in the metal ion reduction during the nanoparticle synthesis.[30] The low acidity of the C-5 hydroxyl group would, therefore, imply negligible chelation at this site. Increased flexibility of the moiety onto which the hydroxyl group is attached would favor metal chelation, in the event of reduced intra/intermolecular hydrogen bonding. We are currently conducting the computational-modeling studies to ascertain the most viable pathway of the proposed QDP–Pd nanoparticle synthesis mechanism.

Also, the palladium(II) ions have a high oxidation–reduction potential that favors the stability of the final step in the nanoparticle synthesis. Concerning these factors, we propose that the most viable palladium(II) ion chelation that will result in nanoparticle formation is the one highlighted in green (Scheme 1). There is a very minimal possibility that the structure

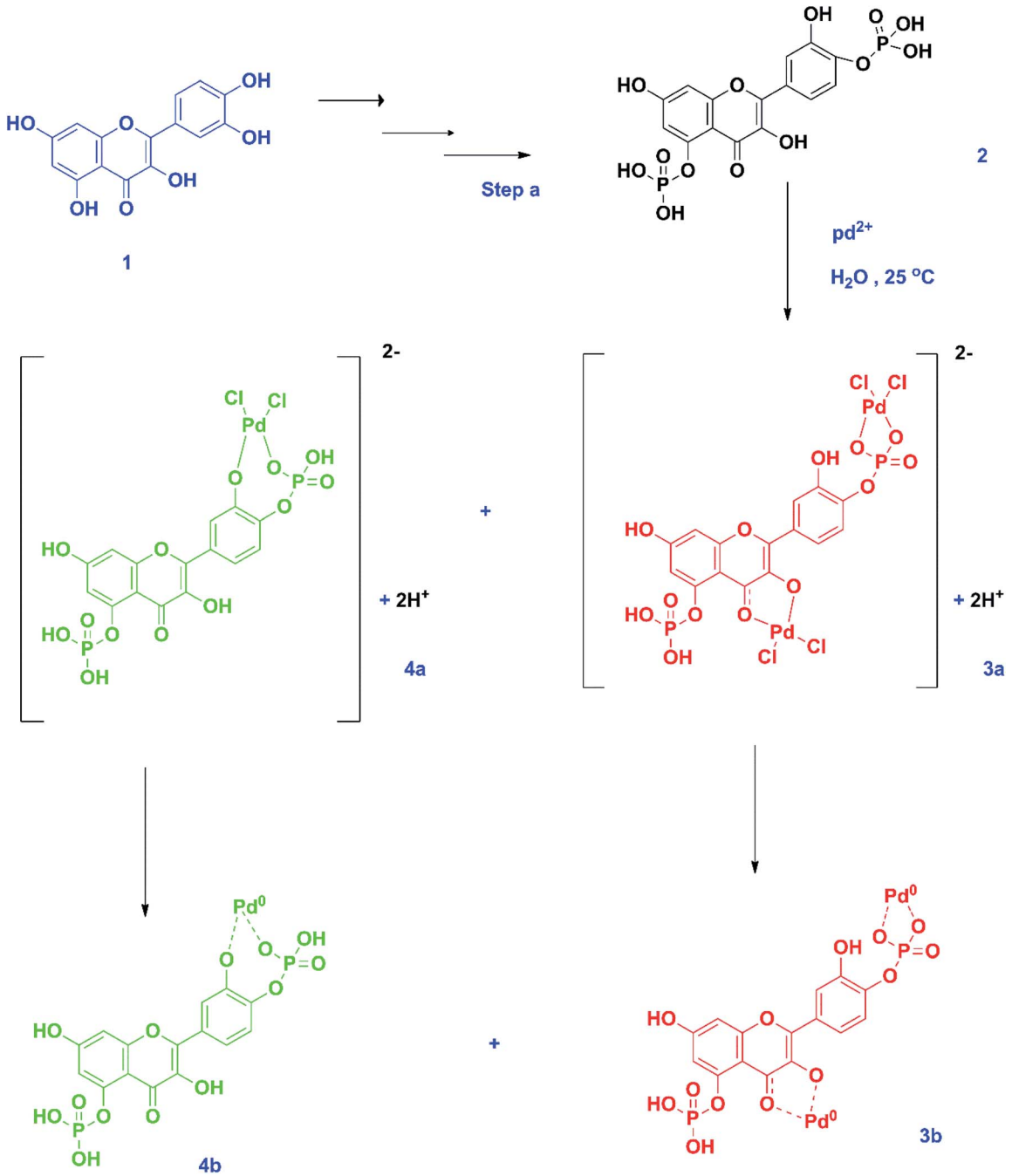

Scheme 1 Synthesis of palladium nanoparticles from QDP and palladium(II) ions. Step a – synthesis of QDP from quercetin,[26] **1** – quercetin, **2** – QDP, **3a** – unfavorable surface complex state, **4a** – favorable surface complex state, **3b** – unfavorable oxidation-reduction state, and **4b** – favorable oxidation-reduction state. Green-favorable state while red-unfavorable but viable state.

highlighted in red would result in a viable/stable nanoparticle formation. Computational studies of the QDP molecule should provide additional information on the charge and steric factors as well as their influence on nanoparticle synthesis.

3.6 Antifungal activity

In this study, two different pathogenic fungi were used to test for antifungal activity of the PdNPs, *C. gloeosporioides*, and *F. oxysporum*. There were 8 different PdNP solutions used in this study. The average sizes for the solutions were 200 nm, 220 nm, 250 nm, 350 nm, 400 nm, 450 nm, 500 nm, and 550 nm for solutions 1 through 8, respectively. For *C. gloeosporioides*, no inhibition zones, IZ, were visible after 1 day of incubation. IZ was visible and measurable for plates containing nanoparticles 1, 2, and 3 after 2 days of incubation as seen in Fig. 7(A). There were colonies, however, within the IZ after 2 days. For FO, IZ were visible and measurable after only 1 day of incubation on plates containing nanoparticle solutions 1, 2, 3, 4, and 8. This is

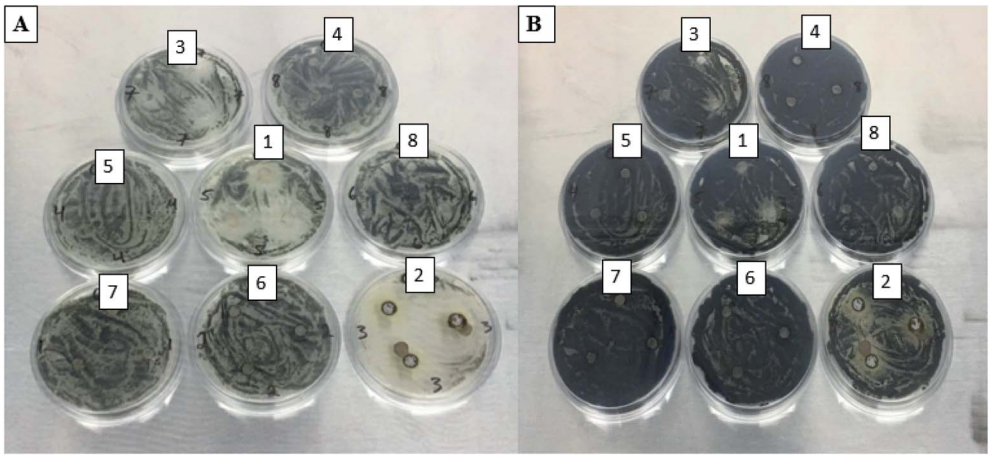

Fig. 7 CG plates for 8 PdNPs solutions after 2 days (A) and CG plates for 8 PdNPs solutions after 4 days (B).

shown in Fig. 8(A). NP1 had the largest inhibition zones on day 4. This is shown in Fig. 8(B). Due to the fungus overcoming the nanoparticles, no IZs were observed on day 7 (Tables 3 and 4).

Palladium nanoparticles are mostly used as catalysts for various reactions.[32,33] Few studies have reported testing the antimicrobial activity of the nanoparticles. Adams *et al.* showed that the small differences in the size of the Pd nanoparticles could significantly affect the antimicrobial properties.[23] These authors reported differences in the antimicrobial activity of the nanoparticles for two different bacteria, *E. coli* and *S. aureus*.[23] In this study, nanoparticles 1 (200 nm), 2 (220 nm), and 3 (250 nm) showed a toxicity for both of the fungi. Nanoparticle 1 (200 nm) was the most effective of the three. It is interesting to note that nanoparticle 4 (350 nm) and 8 (550 nm) exhibited antifungal properties for *F. oxysporum* only. However, NP 5–7 (400 nm, 450 nm, and 500 nm) did not show any antifungal properties. This may be caused by the conglomeration of the nanoparticles and fine-scale (<1 nm) differences in size can alter antimicrobial activity. In this work, it appears that size must not be the only contributing factor for the nanoparticles against *F. oxysporum*. Other factors that could affect the antifungal activity including fine-scale, nutrient composition, and target organisms.

Table 3 Average length of IZ in mm on CG plates after 2 days and 4 days. (NZ = no inhibition zone)

	Day 2 (CG) (mm)	Day 4 (CG) (mm)
1	3.6	1.6
2	7.9	6.3
3	2.4	0.7
4	NZ	NZ
5	NZ	NZ
6	NZ	NZ
7	NZ	NZ
8	NZ	NZ

The exact mechanism for the toxicity of these particles is not known. However, according to our results, the size of the particle plays a significant role in the PdNPs antifungal

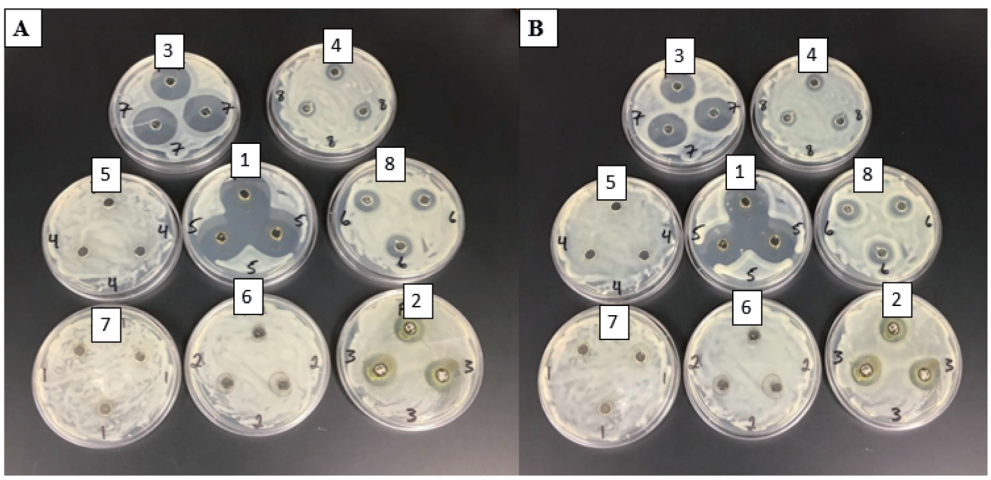

Fig. 8 FO plates for 8 Pd nanoparticle solutions after 1 day (A) and FO plates for 8 Pd nanoparticle solutions after 2 days (B).

Table 4 Average length of IZ in mm on FO plates after 1 day and 2 days. (NZ = no inhibition zone)

	Day 1 (FO) (mm)	Day 2 (FO) (mm)
1	12.2	10.9
2	5.1	4.7
3	10.4	9.6
4	1.5	1.3
5	NZ	NZ
6	NZ	NZ
7	NZ	NZ
8	3.8	3.3

properties. The smallest size nanoparticles (200–250 nm) showed the highest antifungal activity. Adams *et al.* also demonstrated that the size of PdNPs has an impact on their antimicrobial properties.[23] Though Pd nanoparticles' mechanism is not known, Pd^{2+} mechanism is known for a few different pathways. One pathway is in the Fenton reaction. Pd^{2+} will not take the place of iron in this reaction; however, it will cause an increase in hydroxyl radicals. This can cause damage to the cell. Pd^{2+} can also bind to phosphate groups of DNA or other macromolecules on the outside of the cell and cause damage to the cell.[34] Pd^{2+} is also a known enzyme inhibitor. It inhibits creatine kinase, succinate dehydrogenase, alkaline phosphatase, and other enzymatic processes in eukaryotic cells.[35]

4 Conclusion

In this study, the green synthesis and characterization of PdNPs using quercetin derived flavonoid, quercetin di-phosphate (QDP) has been demonstrated. Ultraviolet, visible spectroscopy (UV-vis), X-ray diffraction (XRD), transmission electron imaging (TEM), and EDS results were used to the fullest to determine the reaction efficiency of both QDP and $PdCl_2$ in water-soluble conditions by altering concentrations and temperatures to manipulate and study nanoparticle production. Results yielded support to the claim that increase concentrations of QDP, with respect to a constant $PdCl_2$ ratio, will significantly increase the overall PdNPs production and output. PdNPs synthesized were found to be perfectly spherical and ranged from sizes of 1 nm to 0.6 micrometers. Overall, a clean, non-toxic, biocompatible, efficient, and environmentally friendly method of PdNPs was demonstrated and characterized. The main reducing, stabilizing, and capping agent, quercetin diphosphate (QDP), was shown to be a water-soluble reagent capable of creating nanoparticles of several metals without the need for any unnecessary conditional additions. NPS 1, 2, and 3, with average sizes of 200 nm, 220 nm, and 250 nm, respectively showed the highest antifungal activity for both of the fungi that were tested. The size of the nanoparticles played a significant role against *C. gloeosporioides*, but size did not seem to be the only factor for antifungal properties against *F. oxysporum*. These nanoparticles exhibited fungistatic properties against both of these pathogenic fungi.

Conflicts of interest

There are no conflicts to declare.

Acknowledgements

The authors acknowledge the National Science Foundation Grant # IOS-1543944 and Bill & Melinda Gates Foundation for funding.

References

1 S. Agnihotri, S. Mukherji and S. Mukherji, Immobilized silver nanoparticles enhance contact killing and show highest efficacy: elucidation of the mechanism of bactericidal action of silver, *Nanoscale*, 2013, **5**(16), 7328.
2 M. Darroudi, M. M. Ahmad, A. H. Abdullah, N. A. Ibrahim and K. Shameli, Green synthesis and characterization of gelatin-based and sugar-reduced silver nanoparticles, *Int. J. Nanomed.*, 2011, 569.
3 S. Hrapovic, Y. Liu, K. B. Male and J. H. Luong, Electrochemical Biosensing Platforms Using Platinum Nanoparticles and Carbon Nanotubes, *Anal. Chem.*, 2004, **76**(4), 1083–1088.
4 D. Mukherjee, Potential application of palladium nanoparticles as selective recyclable hydrogenation catalysts, *J. Nanopart. Res.*, 2007, **10**(3), 429–436.
5 H. Chen, G. Wei, A. Ispas, S. G. Hickey and A. Eychmüller, Synthesis of Palladium Nanoparticles and Their Applications for Surface-Enhanced Raman Scattering and Electrocatalysis, *J. Phys. Chem. C*, 2010, **114**(50), 21976–21981.
6 S. Cheong, J. D. Watt and R. D. Tilley, Shape control of platinum and palladium nanoparticles for catalysis, *Nanoscale*, 2010, **2**(10), 2045.
7 K. R. Gopidas, J. K. Whitesell and M. A. Fox, Synthesis, Characterization, and Catalytic Applications of a Palladium-Nanoparticle-Cored Dendrimer, *Nano Lett.*, 2003, **3**(12), 1757–1760.
8 M. Enneiymy, C. Le Drian and J.-M. Becht, Green reusable Pd nanoparticles embedded in phytochemical resins for mild hydrogenations of nitroarenes, *New J. Chem.*, 2019, **43**, 17383–17389.
9 V. L. Nguyen, D. C. Nguyen, H. Hirata, M. Ohtaki, T. Hayakawa and M. Nogami, Chemical synthesis and characterization of palladium nanoparticles, *Adv. Nat. Sci.: Nanosci. Nanotechnol.*, 2010, **1**(3), 035012.
10 Y. Sekiguchi, Y. Hayashi and H. Takizawa, Synthesis of Palladium Nanoparticles and Palladium/Spherical Carbon Composite Particles in the Solid–Liquid System of Palladium Oxide–Alcohol by Microwave Irradiation, *Mater. Trans.*, 2011, **52**(5), 1048–1052.
11 I. Saldan, Y. Semenyuk, I. Marchuk and O. Reshetnyak, Chemical synthesis and application of palladium nanoparticles, *J. Mater. Sci.*, 2015, **50**(6), 2337–2354.
12 R. K. Petla, S. Vivekanandhan, M. Misra, A. K. Mohanty and N. Satyanarayana, Soybean (Glycine Max) Leaf Extract Based

Green Synthesis of Palladium Nanoparticles, *J. Biomater. Nanobiotechnol.*, 2012, **03**(01), 14–19.

13 S. Gurunathan, E. Kim, J. Han, J. Park and J. Kim, Green Chemistry Approach for Synthesis of Effective Anticancer Palladium Nanoparticles, *Molecules*, 2015, **20**(12), 22476–22498.

14 A. Kanchana, S. Devarajan and S. R. Ayyappan, Green synthesis and characterization of palladium nanoparticles and its conjugates from solanum trilobatum leaf extract, *Nano-Micro Lett.*, 2010, **2**(3), 169–176.

15 D. Sheny, D. Philip and J. Mathew, Rapid green synthesis of palladium nanoparticles using the dried leaf of Anacardium occidentale, *Spectrochim. Acta, Part A*, 2012, **91**, 35–38.

16 X. Yang, Q. Li, H. Wang, J. Huang, L. Lin, W. Wang and L. Jia, Green synthesis of palladium nanoparticles using broth of Cinnamomum camphora leaf, *J. Nanopart. Res.*, 2009, **12**(5), 1589–1598.

17 T. Sun, Z. Zhang, J. Xiao, C. Chen, F. Xiao, S. Wang and Y. Liu, Facile and Green Synthesis of Palladium Nanoparticles-Graphene-Carbon Nanotube Material with High Catalytic Activity, *Sci. Rep.*, 2013, 3.

18 V. A. Okello, F. J. Osonga, M. T. Knipfing, V. Bushlyar and O. A. Sadik, Reactivity, characterization of reaction products and immobilization of lead in water and sediments using quercetin pentaphosphate, *Environ. Sci.: Processes Impacts*, 2016, **18**(3), 306–313.

19 F. J. Osonga, V. M. Kariuki, I. Yazgan, A. Jimenez, D. Luther, J. Schulte and O. A. Sadik, *Sci. Total Environ.*, 2016, **563**, 977–986.

20 F. J. Osonga, I. Yazgan, V. Kariuki, D. Luther, A. Jimenez, P. Le and O. A. Sadik, Greener synthesis and characterization, antimicrobial and cytotoxicity studies of gold nanoparticles of novel shapes and sizes, *RSC Adv.*, 2016, **6**(3), 2302–2313.

21 K. Tahir, S. Nazir, A. Ahmad, B. Li, S. A. A. Shah, A. U. Khan, G. M. Khan, Q. U. Khan, Z. U. H. Khan and F. U. Khan, Biodirected synthesis of palladium nanoparticles using Phoenix dactylifera leaves extract and their size dependent biomedical and catalytic applications, *RSC Adv.*, 2016, **6**, 85903.

22 N. S. Al-Radadi and R. M. Ramadan, Synthesis and characterization of new binary and ternary palladium and platinum complexes affective to antitumor, *Eur. Sci. J.*, 2014, **10**, 44–58.

23 C. P. Adams, K. A. Walker, S. O. Obare and K. M. Docherty, Size-dependent antimicrobial effects of novel palladium nanoparticles, *PLoS One*, 2014, **9**, 1–12.

24 A. Viswadevarayalu, P. V. Ramana, J. Sumalatha and S. A. Reddy, Biocompatible synthesis of palladium nanoparticles and their impact on fungal species, *J. Nanosci. Nanotechnol.*, 2016, **2**, 169–172.

25 R. Dean, J. A. L. Van Kan, Z. A. Pretorius, K. E. Hammond-Kosack, A. D. Pietro, P. D. Spanu, J. J. Rudd, M. Dickman, R. Kahmann, J. Ellis and G. D. Foster, The top 10 fungal pathogens in molecular plant pathology, *Mol. Plant Pathol.*, 2012, **13**, 414–430.

26 F. J. Osonga, J. O. Onyango, S. K. Mwilu, N. M. Noah, J. Schulte, M. An and O. A. Sadik, Synthesis and characterization of novel flavonoid derivatives via sequential phosphorylation of quercetin, *Tetrahedron Lett.*, 2017, **58**, 1474–1479.

27 M. Balouiri, M. Sadiki and S. K. Ibnsouda, Methods for in vitro evaluating antimicrobial activity: a review, *J. Pharm. Anal.*, 2016, **6**, 71–79.

28 M. Khan, M. Khan, M. Kuniyil, S. F. Adil, A. A-Warthan, H. Z. Alkhathlan, W. Tremel, M. N. Tahir and R. H. Siddiqui, Biogenic synthesis of palladium nanoparticles using Pulicaria glutinosa extract and their catalytic activity towards the Suzuki coupling reaction, *Dalton Trans.*, 2014, **43**, 9026–9031.

29 P. Dauthal and M. Mukhopadhyay, Biosynthesis of palladium nanoparticles using Delonix regia leaf extract and its catalytic activity for nitro-aromatics hydrogenation, *Ind. Eng. Chem. Res.*, 2013, **52**(51), 18131–18139.

30 M. Can, Green Synthesis of Pd Nanoparticles via Gallic Acid, *Acta Phys. Pol., A*, 2017, **131**(3), 569–570.

31 K. E. Heim, A. R. Tagliaferro and D. J. Bobilya, Flavonoid antioxidants: chemistry, metabolism and structure-activity relationships, *J. Nutr. Biochem.*, 2002, **13**(10), 572–584.

32 Y. Li, X. M. Hong, D. M. Collard and M. A. El-Sayed, Suzuki Cross-coupling Reaction Catalyzed by Palladium Nanoparticles in Aqueous Solution, *Org. Lett.*, 2000, **2**(15), 2385–2388.

33 M. Yu, L. Yan, P. Frank and B. Matthias, Catalytic activity of palladium nanoparticles encapsulated in spherical polyelectrolyte brushes and core-shell microgels, *Chem. Mater.*, 2007, **19**(5), 1062–1069.

34 T. Z. Liu, T. F. Lin, D. T. Y. Chiu, K.-J. Tsai and A. Stern, Palladium or Platinum Exacerbates Hydroxyl Radical Mediated DNA Damage, *Free Radicals Biol. Med.*, 1997, **23**(1), 155–161.

35 T. Z. Liu, S. D. Lee and R. S. Bhatnagar, Toxicity of Palladium, *Toxicol. Lett.*, 1979, **4**(6), 469–473.

